

# Candidate Hippocampal Biomarkers of Susceptibility and Resilience to Stress in a Rat Model of Depression\*<sup>§</sup>

Kim Henningsen<sup>‡||\*\*</sup>, Johan Palmfeldt<sup>§\*\*</sup>, Sofie Christiansen<sup>‡</sup>, Isabel Baiges<sup>§</sup>, Steffen Bak<sup>¶||‡‡</sup>, Ole Nørregaard Jensen<sup>‡‡</sup>, Niels Gregersen<sup>§</sup>, and Ove Wiborg<sup>‡</sup>

**Susceptibility to stress plays a crucial role in the development of psychiatric disorders such as unipolar depression and post-traumatic stress disorder. In the present study the chronic mild stress rat model of depression was used to reveal stress-susceptible and stress-resilient rats. Large-scale proteomics was used to map hippocampal protein alterations in different stress states. Membrane proteins were successfully captured by two-phase separation and peptide based proteomics. Using iTRAQ labeling coupled with mass spectrometry, more than 2000 proteins were quantified and 73 proteins were found to be differentially expressed. Stress susceptibility was associated with increased expression of a sodium-channel protein (SCN9A) currently investigated as a potential antidepressant target. Differential protein profiling also indicated stress susceptibility to be associated with deficits in synaptic vesicle release involving SNCA, SYN-1, and AP-3. Our results indicate that increased oxidative phosphorylation (COX5A, NDUFB7, NDUFS8, COX5B, and UQCRB) within the hippocampal CA regions is part of a stress-protection mechanism. *Molecular & Cellular Proteomics* 11: 10.1074/mcp.M111.016428, 1–12, 2012.**

Stress exposure can lead to serious illnesses such as depression and post-traumatic stress disorder and have fatal consequences (1–3). However, some individuals are able to cope with even severe stressors and seem to be stress resilient (4, 5). It is widely accepted that resiliency is not merely a lack of stress susceptibility, but it is an active process involving physiological as well as psychological adaptations. The resilience phenotype is important, both with respect to discovering biomarkers to the pathological state distinctly asso-

ciated with stress susceptibility and with regard to understanding of the biological underpinnings for resiliency.

The hippocampal formation is involved in the stress response as a vital part of the negative feedback system regulating circulating glucocorticoids (6, 7). Moreover, the hippocampus is coupled to stress through fear and emotional processing via its connections to the amygdala (8, 9). The hippocampal formation is believed to be implicated in the etiology of depression, potentially through an important role in stress responses (10–12). Based on the role of the hippocampal formation in stress and stress-related psychiatric disorders, one might expect to find markers of stress-susceptibility/resilience in this region of the brain.

The development of the chronic mild stress (CMS)<sup>1</sup> rat model of depression was based on the rationale that stress can induce depression (13, 14). The model fulfills all standard validity criteria and has a face validity including several symptoms of depression, with anhedonia as hallmark symptom of the disease (15). Anhedonia is defined as a lack of interest in otherwise pleasurable events or stimuli. In rodents exposed to the CMS regime this symptom appears as decreased reward sensitivity, measured as a reduced sucrose consumption/preference (16, 17) or increased threshold to intercranial self-stimulation (18).

Using the CMS paradigm we have repeatedly found that the majority of rats exposed to chronic mild stress show a gradual reduction in consumption of sucrose solution, indicating an anhedonic-like state. The remaining rats do not reduce their sucrose intake and appear resilient to the stress-induced effects on sucrose intake (17, 19, 20).

From the <sup>‡</sup>Centre for Psychiatric Research, Institute of Clinical Medicine, Aarhus University Hospital, University of Aarhus, Risskov, Denmark; <sup>§</sup>Research Unit for Molecular Medicine, Institute of Clinical Medicine, Aarhus University Hospital, University of Aarhus, Aarhus N, Denmark; <sup>¶</sup>Diabetes Research Centre, Department of Endocrinology, Odense University Hospital, Odense, Denmark; <sup>||</sup>Department of Biochemistry and Molecular Biology, University of Southern Denmark, Odense M, Denmark

Received December 14, 2011

Published, MCP Papers in Press, February 6, 2012, DOI 10.1074/mcp.M111.016428

<sup>1</sup> The abbreviations used are: CMS, chronic mild stress; CA, cornu ammonis; DG, dentate gyrus; iTRAQ, isobaric tag for relative and absolute quantitation; SRM, selected reaction monitoring; BDNF, brain derived neurotrophic factor; VEGF, vascular endothelial growth factor; SCN9A or Na<sub>v</sub>1.7, sodium channel protein; CADPS2, calcium-dependent activator for secretion protein 2; ENSA, alpha-endosulfine protein; SNAP91 or AP180, clathrin coat assembly protein; SNCA, alpha-synuclein; SYN-1, synaptogyrin 1; AP-3, adaptor-related protein complex 3; GABA, gamma-aminobutyric acid; COX5A,B, cytochrome c oxidase subunit 5A,B; NDUFB7, NADH dehydrogenase (ubiquinone) 1 beta subcomplex, 7; UQCRB, ubiquinol-cytochrome c reductase binding protein.

## Study design

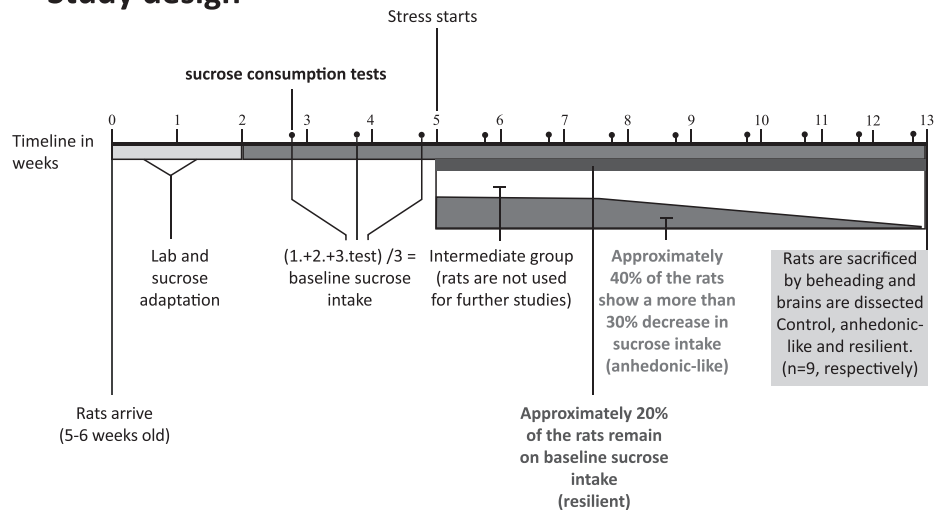


FIG. 1. Study design showing the experiment lineout and time course.

In the present study the aim was to search for proteins linked to the stress-susceptible (termed anhedonic) and stress-resilient phenotype within the hippocampal cornu ammonis (CA) region. The results showed that the anhedonic and resilient phenotypes were associated with distinct protein regulation patterns. In particular, in the resilient group, a large number of proteins were regulated, demonstrating that resiliency implies molecular plasticity within the CA region. In stress-susceptible rats a sodium channel, currently investigated as a novel antidepressant target, was up-regulated. Moreover, expression levels of proteins involved in vesicular release/turnover differed significantly between stress susceptible and stress resilient groups, indicating a potential deficit in vesicle turnover in stress-susceptible rats. Finally, a comparison of control and stress-resilient rats revealed mitochondrial oxidative phosphorylation as a potential mechanism underlying resiliency.

## EXPERIMENTAL PROCEDURES

**Subjects**—Male Wistar rats (Taconic M&B, Ry, Denmark) were used in the study. The initial experimental group contained 300 rats. Twenty-seven rats were used in the main large-scale proteomics study and in the validation study, respectively. Rats were grouped into three categories, based on criteria of behavior during stress experiments. The animals were singly housed, food and water was available *ad libitum*, and animals were kept on a standard 12-h light/dark cycle except when one of these parameters was changed because of the stress regime. All animal procedures were approved by the Danish National Committee for Ethics in Animal Experimentation (2008/561–447).

**Sucrose Consumption Test**—Initially, the animals were trained to consume a palatable sucrose solution (1.5%). The training continued for 5 weeks, with sucrose test conducted twice a week during the first 3 weeks and once a week during the last 2 weeks. Animals were food and water deprived 14 h before the test, which consisted of 1-hour free access to a bottle with sucrose solution. Sucrose consumption was measured by weighing the bottles at the beginning and end of the test. During the stress period, the sucrose consumption test was performed once a week. Independent of the sucrose consumption

test, water intake was monitored once a week by weighing the water bottles before and after a 24 h period. Rats with a mean sucrose intake below 8.5 g were designated as innate low-drinkers and were not used for further experiments. A mean baseline standard deviation (S.D.) was calculated from the total population. Rats with a sucrose-intake S.D. more than twofold above the mean S.D. were excluded from the experiment, to avoid subjects with unstable sucrose intake. Baseline sucrose consumption was defined as the mean sucrose consumption during three sucrose tests conducted before stress initiation. Rats were allocated into experimental groups based on their baseline sucrose intake. Following exposure to stress, rats were characterized as anhedonic (defined as a >30% within-subject decrease in sucrose intake) or resilient (defined as a < 10% within subject decrease in sucrose intake). Rats not corresponding to either criterion were excluded from the experiment (see Fig. 1, showing study design).

**Chronic Mild Stress**—On the basis of sucrose intakes in the three final baseline tests, animals were divided into two groups and placed in separate rooms. One group was exposed to 8 weeks of chronic mild stressors and the other was left unchallenged. The unchallenged group was food and water deprived 14 h before sucrose consumption test only.

The stress protocol consisted of seven different stress conditions each lasting 10 to 14 h. One period of intermittent illumination, stroboscopic light, grouping, food or water deprivation, and two periods of soiled cage and no stress, and three periods of 45° cage-tilting.

**Tissue Processing**—Animals were decapitated and the brains were immediately dissected. The hippocampi were removed and subdivided to yield the CA1 and CA3 subregion according to a method reported in detail elsewhere (21). These two regions were pooled and were immediately snap-frozen before used in the proteome analysis. Proteome analysis was conducted on three sample pools corresponding to three rats in each treatment group, respectively.

**Immunohistochemistry**—After an intraperitoneal overdose of sodium pentobarbital (60 mg/ml, 100 mg/kg) the rats were transcardially perfused with 100 ml 0.9% saline, followed by 200 ml of ice cold 4% paraformaldehyde (pH 7.2–7.4). The brains were removed from the skull and the right hemisphere was postfixed overnight in the same solution at 4 °C. The brains were transferred to a solution consisting of 30% sucrose (diluted in phosphate buffer, pH 7.0–7.4) supplemented with 10% sodium azide and stored at 4 °C until they sank.

The brains were sectioned sagittally on a cryostat (Leica, 3050 CS). The 40  $\mu\text{m}$  sections were collected in series of every 10 (~120 sections per brain) and were stored in cryoprotectant antifreeze solution (25% ethylene glycol and 25% glycerin in a 0.05 M phosphate-buffered saline (PBS)) at  $-20^\circ\text{C}$ .

The sections were rinsed in cold 0.1% PBS ( $3 \times 10$  min.). To detect antigens, the sections were incubated 1 h at  $95^\circ\text{C}$  in 1 mM Tris, pH 9, supplemented with 0.5 mM EGTA. Nonspecific binding of immunoglobulin was quenched by incubating the sections in 50 mM  $\text{NH}_4\text{Cl}$  (30 min.) and were blocked in PBS supplemented with 1% bovine serum albumin (BSA), 0.01% Triton X 100, and 0.2% gelatin ( $3 \times 20$  min.). Incubation with the primary antibody (Nav1.7, ab65167, Abcam (Cambridge, UK), 1:500) diluted in PBS and supplemented with 0.1% BSA and 0.01% Triton X100 was done overnight at  $+4^\circ\text{C}$ . To control for nonspecific staining, some of the sections were incubated without primary antibody.

The sections were rinsed in 0.1% BSA, 0.2% gelatin, 0.1% Triton X100 in PBS ( $3 \times 10$  min) and were incubated with the secondary antibody (Goat, anti-rabbit IgG coupled to Alexa 488, 1:2000) diluted in 0.1% BSA, 0.3% Triton X 100 in PBS for 1 h at room temperature followed by rinsing in PBS ( $2 \times 5$  min.). The sections were then mounted with a coverslip in Glycergel antifade medium (Dako) and were inspected on Zeiss Axiovert 200 M fluorescence microscope using Neofluar  $10 \times$  objective.

**Proteome Fractionation**—Rat brain tissue was homogenized with a Potter-Elvehjem in cold lysis buffer (10 mM Hepes, pH 7.2, with complete protease inhibitors (Roche Diagnostics)), sonicated three times for 10 s, and briefly centrifuged ( $400 \times g$ , 5 min,  $4^\circ\text{C}$ ) to remove tissue particles and cell debris. The supernatant from homogenization was ultracentrifuged ( $120,000 \times g$ , 60 min.,  $4^\circ\text{C}$ ) to separate the membranes from the new supernatant (S). The membrane pellet was washed in sodium carbonate buffer (22) to remove contaminant soluble proteins and thereafter ultracentrifuged again. The new membrane pellet was further purified by dissolving it in Triton X-114 buffer and separating the proteins into two phases as previously described (23–25). Briefly, pellets of membrane proteins were dissolved on ice in ~1% Triton X-114. After 15 min incubation at  $30^\circ\text{C}$  a bottom phase of Triton-X114 micelles was formed and collected after centrifugation ( $1300 \times g$ , 10 min). The Triton-X114 detergent phase, mostly containing membrane proteins (M) and the S sample were purified by precipitation and further analyzed by proteomics as previously described (25).

**Peptide Labeling and Fractionation**—The labeling procedure was performed three times corresponding to biological triplicates of S and M fraction. For each triplicate samples from three animals were pooled (33  $\mu\text{g}$  of peptides each) and each of the resulting 100  $\mu\text{g}$  peptide sample was labeled with a different isobaric tag for relative and absolute quantitation (iTRAQ) reagent in accordance with the manufacturer's instructions (Applied Biosystems, Foster City, CA). Random swapping of iTRAQ labels was applied in the different replicate studies to avoid possible label-specific effects. The subsequent analytical steps were performed as previously described (25). Labeled peptides were mixed and purified on a strong cation exchange chromatography column followed by elution with volatile buffer containing 5% ammonia and 30% methanol. Pure peptides were dried and resuspended in denaturing buffer. The peptides were separated on an Immobiline Drystrip gel (GE Healthcare, Uppsala, Sweden) using isoelectric focusing on a Multiphor II unit (Pharmacia Biotech AB, Uppsala, Sweden). The pH range was 3.5–4.5 for S peptides and 3–10 for M peptides. The gel strip was cut into 12 pieces and the peptides were extracted from the gel in two steps with 0.5% trifluoroacetic acid in 5% acetonitrile (ACN). Peptides were vacuum-dried and re-dissolved in 0.5% trifluoroacetic acid in 5%

ACN. Peptides were purified on PepClean C-18 Spin Columns (Pierce, Rockford, IL) according to manufacturer's protocol prior to nanoLC-MS/MS analysis.

**Nano-liquid Chromatography and MS Analysis**—The peptide mixtures were separated by liquid chromatography (Easy nLC from Proxeon, Odense, Denmark) coupled to mass spectrometry (LTQ-Orbitrap, Thermo Fisher Scientific, Waltham, MA) through a nano-electrospray source with stainless steel emitter (Proxeon, Odense, Denmark). The peptides were separated on a reverse phase column, 75  $\mu\text{m}$  in diameter and 100 mm long, packed with 3.5  $\mu\text{m}$  Kromasil C18 particles (Eka Chemicals, Bohus, Sweden) at a flow of 300 nL/minute using a 100 min gradient of ACN in 0.4% acetic acid, starting with 5% and ending with 35% ACN. The mass spectrometry detection was full scan ( $m/z$  400–2000) with Orbitrap detection at resolution  $r = 60,000$  (at  $m/z$  400) followed by up to four data-dependent MS/MS scans, with linear ion trap (LTQ) detection of the most intense ions. Dynamic exclusion of 25 s was employed as well as rejection of charge state +1. Pulsed Q dissociation (PQD) fragmentation was performed with activation time of 0.1 s, normalized collision energy of 33, and activation Q of 0.7.

**Database Searches and Statistics**—The raw data files were processed using extract\_msn.exe (Thermo Fisher Scientific, released 2/15/2005) to generate peak lists of the tandem spectra. The processed data were searched with Mascot ([www.matrixscience.com](http://www.matrixscience.com)) version 2.2.04 (Matrix Science, London, UK), which was used for protein identification and iTRAQ reporter quantification. In each study, the twelve different peptide fractions were MS-analyzed in duplicate and all generated peak lists were merged. The merged files were searched against the IPI\_rat\_20090423 database with 39879 sequences using the MudPIT scoring algorithm of Mascot. Full scan tolerance was 5 ppm and MS/MS tolerance was 0.75 Da. Setting of trypsin digestion was cleavage at C-terminal of lysine and arginine except before proline, and up to two missed cleavages were accepted. Fixed modifications were those originating from iTRAQ protocol: iTRAQ-4plex of lysine and N-terminal and methylthio modification of cysteines, whereas oxidation of methionine and iTRAQ-4plex of tyrosine were set as variable modifications. The significance level of protein identifications was set to 0.001, which resulted in a false discovery rate of less than 0.003 when searched in Mascot against the decoy database of random sequences. Throughout the manuscript, the HGNC symbol (<http://www.genenames.org/>) obtained from the IPI-database was used to refer to protein hits. iTRAQ values were reported for proteins with five or more measured iTRAQ scan values from at least two peptides, each with an expectation value of 0.02 or below.

iTRAQ quantitation was performed in Mascot where normalization to summed intensities was applied to compensate for possible variation in starting material. For details, see [http://www.matrixscience.com/help/quant\\_config\\_help.html](http://www.matrixscience.com/help/quant_config_help.html). When identification of a protein yielded several possible protein isoforms, all of them were considered for quantification. In the quantitative calculations, only protein isoforms with iTRAQ values in all three analyses were included. All MS data are available in PRIDE database with Accession numbers: 19005–19010. WebStart URL: <http://tinyurl.com/3kd7>  $\times$  44 (26).

The iTRAQ-ratios between the experimental groups were calculated for each protein from the three independent studies giving independent triplicate values (e.g. three separate values of C/A values). Ratios for each protein were reported as significantly different from 1.0 if they passed two tests: (1) a fold change criterion of two times the global standard error ( $2 \times 0.09 = 0.18$ ) and (2) a two-tailed student's *t* test for equal variance data. False discovery rate (FDR) for differential expression was calculated to be ~18% using Benjamini and Hochberg's statistics with extra stringency from the fold change criterion (27, 28). Differences in sucrose consumption were tested

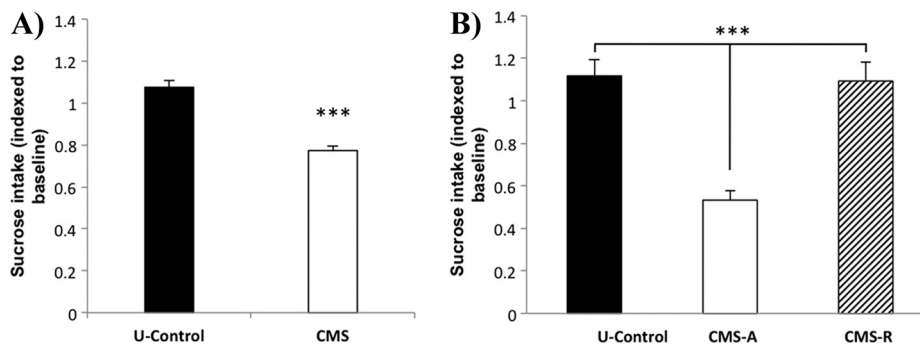


FIG. 2. **A**, Four weeks exposure to chronic mild stress (CMS) resulted in a significantly decreased sucrose consumption when compared with unchallenged controls (C) ( $n = 72$ – $164$ ). **B**, Seven weeks of stress resulted in a significant decrease in sucrose consumption in stress-susceptible rats (A). A subgroup of the stressed rats did not decrease sucrose intake (R). ( $n = 9$ ), (\*\*\*) =  $p < 0.001$ ). Data are shown as sucrose intake, indexed to baseline (3–4 week and 7–8 week means) + standard error to the mean.

with Student's *t*-test or One-Way ANOVA followed by bonferroni's correction when three groups were being compared.

**Selected Reaction Monitoring (SRM)**—Nine proteins were selected for validation by SRM analysis of material from new rat specimens (nine rats from each treatment group) prepared with the same procedures as in the main large scale proteomics study. At least three proteotypic peptides for each protein were SRM analyzed. Isotopically labeled, heavy versions of all the selected peptides were synthesized (JPT Peptide Technologies GmbH), and added to each sample. The digested peptides were resuspended in 0.1% formic acid. Approximately 1  $\mu$ g peptides were used for each SRM run. The peptides were loaded onto an EASY-nano LC system (Thermo Fisher Scientific). The peptides were trapped on a 2 cm 100  $\mu$ m inner diameter, 360  $\mu$ m outer diameter, ReproSil - Pur C18 AQ 5  $\mu$ m (Dr. Maisch, Ammerbuch-Entringen, Germany) and separated using a 15 cm 75  $\mu$ m inner diameter, 360  $\mu$ m outer diameter, ReproSil - Pur C18 AQ 3  $\mu$ m (Dr. Maisch) reversed phase capillary column. The peptides were eluted using a gradient from 0% to 34% phase B (0.1% formic acid, 90% ACN) over 34 min at 250 nL/min directly into a triple quadrupole mass spectrometer (TSQ Vantage, Thermo Scientific, San Jose, CA). The TSQ Vantage was operated in a nano-electrospray mode. For ionization, 2300 V of spray voltage and 200 °C capillary temperature were used. The selectivity for Q1 was set to 0.7 and Q3 at 0.7 Da (FWHM). The collision gas pressure of Q2 was set at 1.5 mTorr argon. The collision energies were calculated by Pinpoint 1.1 (Thermo Scientific). The instrument acquisition was performed in SRM mode using an overall cycle time of 2 s. A total of 410 transitions were used for targeting the 41 heavy and 41 light peptides divided into windows of 8 min. All raw files were processed by Pinpoint 1.1. The targeted peptides were verified by comparing transition intensities and retention times between the light and heavy form. For each targeted peptide that fulfilled the verification criteria, the software computed the integrated peak areas of the transition ions and normalized it to the signal from its corresponding heavy standard form. Two household proteins (Glyceraldehyde-3-phosphate dehydrogenase and 60S ribosomal protein L23) were used for internal normalization.

**Protein Classification and Pathway Analysis**—Proteins that passed significance criteria were arranged according to function and process. Protein function and process was inferred from the IPI database (<http://www.ebi.ac.uk/IPI/IPIhelp.html>) and literature searches ([www.ingenuity.com](http://www.ingenuity.com)).

**Cluster Analysis**—Cluster analysis was used to separate the three groups based on between-group similarities in global protein expression profiles. The clustering approach orders objects in a treelike structure and provides information about relations among groups.

The cluster analysis was performed with Cluster software version 2.11 (29). Hierarchical clustering was performed by clustering genes and arrays. Subsequently, the cluster analysis was visualized by Tree View software version 1.60 (<http://rana.lbl.gov/EisenSoftware.htm>).

## RESULTS

**Sucrose Consumption**—Sucrose consumption was applied to assess stress-induced anhedonic-like and resilient behavior of rats. The data of the groups was normally distributed (as tested by Q-Q-plots). Moreover, no statistically significant difference between the groups indicated that they were well-matched (data not shown). Three-weeks exposure to CMS ( $n = 164$ ) resulted in significantly decreased sucrose consumption when compared with unchallenged controls ( $n = 72$ ) ( $p < 0.00001$ ). Fig. 2A shows the mean group sucrose intake indexed to baseline values.

Forty-three percent of the stressed rats showed a more than 30% decrease in sucrose intake and were defined as anhedonic-like. On the other hand, 23% of the rats exposed to stress did not decrease their sucrose intake and were designated stress resilient. Unchallenged rats did not decrease their sucrose intake. A subset of the unchallenged controls (C), anhedonic-like (A) and resilient (R) rats (nine in each group) were used for the proteome analysis. Fig. 2B shows the sucrose intake (indexed to baseline) of the rats used for proteome analysis.

To confirm that the decrease in sucrose consumption was linked to palatable sucrose and not to general physiology, a 24-hour water consumption was measured once weekly during the experiment in a subset of the control and stress group ( $n = 20$  for each group). No differences were found in water consumption, with both the control and stress group having a 24-hour mean water consumption of 39 ml (data not shown).

**Proteome and Cluster Analysis**—Large scale protein analysis was performed on hippocampi from the control, anhedonic-like, and stress resilient rats to identify proteins differentially expressed in the three groups. Quantitative data were obtained for 1199 and 1054 proteins from the membrane and soluble sample, respectively, with 242 proteins detected in

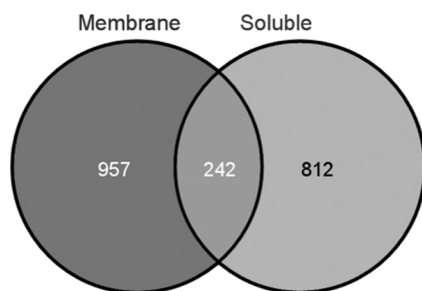


FIG. 3. Quantitative data were obtained for 1199 and 1054 proteins from the membrane and soluble sample, respectively, with 242 proteins detected in both fractions.

both fractions (Fig. 3). Extensive lists of proteins with quantitative data are in [Supplemental Tables S1 to S3](#), and detailed identification data are in [Supplemental Table S4 to S5](#).

Out of the 2011 unique protein hits, the main focus was set on those proteins that passed statistical tests. Three experimental groups of rats were analyzed (with triplicates from each, and each triplicate was a mixture from three independent rats): Unchallenged Control (C), Anhedonic-like (A), and CMS-Resilient (R). Table I shows the number of significant protein hits (either down- or up-regulated) for the respective sample comparisons. Seventy-three proteins were significantly altered between the groups (Table II).

Two separate cluster analyses were performed. One was performed on data from all 2011 proteins and another was performed on the 73 proteins that passed selection criteria. According to both cluster profiles, the resilient group diverged from the anhedonic and control group, demonstrating that the protein expression profile of the resilient group differed from the other two groups investigated (Figs. 4A and 4B).

**SRM**—We conducted a validation experiment using subgroups identical to the original experiment and the SRM method to validate the results obtained using iTRAQ labeling. Nine proteins were selected for validation. Two proteins from the soluble sample and seven from the membrane sample. Only one peptide was detected for the Gng-2 protein and therefore this protein was excluded from further analysis. The two proteins from the soluble sample, Pgl-6 and Ap3d1 did not show differential expression levels comparable to the results from the iTRAQ experiment. Differential regulation in line with iTRAQ data was confirmed in five of six proteins, namely Scn9a, Slc1a4, Snca, Syng1, and Tmpo. Regulation of Cacna1b was not confirmed. A study comparison is shown in Fig. 5.

**Histology**—We assessed the presence of the SCN9A protein (Nav1.7) in the hippocampus by staining this sodium channel in cryocut brain sections (Fig. 6). In control rats, we found highest immunoreactivity in the CA3, with lower intensities in the CA1, and very little reactivity in the DG. We observed higher immunoreactivity in anhedonic rats compared with controls, especially pronounced in the CA1 region. This observation confirmed the results from the proteome experi-

TABLE I

The number of significant protein hits (down or up-regulated) for the respective sample comparisons. Control (C), Anhedonic (A), Resilient (R)

	Proteins differentially regulated		
	C vs. A	R vs. A	C vs. R
Up	10	17	3
Down	12	15	16
Total	22	32	19

ment, showing increased Nav1.7 expression in anhedonic rats compared with controls. Immunoreactivity was confirmed in the dorsal root ganglia, a neural area known to contain a large density of Nav1.7.

#### DISCUSSION

By exposing rats to the CMS regime, we obtained rat groups with different stress response phenotypes, using sucrose consumption as readout on hedonic-like status. The hippocampal proteome was analyzed by mass spectrometry-based proteomics and numerous proteins, differentially expressed in the different stress-response phenotypes, were identified. More than 2000 proteins were detected using a two-phase fractionation method designed to facilitate detection of membrane proteins (25). This method proved highly successful with 957 proteins being classified as associated to membranes, a protein group likely to be involved in cell signaling.

We have previously reported that, rats exposed to CMS, show a graded response to stress, using sucrose-intake as behavioral readout (17, 19, 20, 30). This finding was reproduced in the present study, which showed a general effect of 4 weeks of mild stress exposure on sucrose intake with a mean decrease of 23% (Fig. 2A) and no concurrent reduction of water intake. The sucrose consumption data follow a right-skewed normal distribution, thus the definition as anhedonic and resilient rats respectively is based on an operational cutoff chosen by the experimenter. A graded effect of stress exposure is expected and a distinction into stress-susceptible and stress-resilient rats provides a useful approach for identifying potential biomarkers specific for anhedonia, as opposed to general stress effects. Moreover, inclusion of the resilience group improves the translational value of the CMS model, as stress resiliency is a common clinical phenomenon (31). Furthermore, data from the resilient group might shed light on novel treatment opportunities augmenting resiliency. Recently, a resilience phenotype has also been described in studies employing the chronic social defeat model of depression (32, 33) and stress susceptibility/resilience has also been assessed following exposure to cold-swim-stress (34) further arguing for the importance of this subgroup.

The aim of the present study was to determine whether proteome changes in the rat hippocampal CA-subregion following exposure to CMS correlate reliably with stress-sus-

## Hippocampal Biomarkers of Stress Susceptibility

TABLE II

A, Table II (A, B, and C) List of proteins significantly altered between groups. Ratios for each protein was reported as significantly different from 1.0 if they passed two tests 1) a threshold test of two times the global standard error ( $2 \times 0.09 = 0.18$ ) and 2) a two-tailed student's T-test for equal variance data. A) Control vs. Anhedonic. B) Resilient vs. Anhedonic. C) Control vs. Resilient

Fraction	IPI number	Abbreviation	Protein description	Function description	Process	C vs A
M	IPI00369419	-	Uncharacterized cofilin-like/ 19 kDa protein	Cytoskeleton	Actin binding	0.76
S	IPI00365286	Vcl	Vinculin	Cytoskeleton	Protein binding	0.79
M	IPI00870837	Mlc1	Megalencephalic leukoencephalopathy 1	Ion channel	Membrane ion Channel	0.76
M	IPI00480827	Scn9a	Sodium channel protein type 9 alpha	Ion channel	Sodium ion transport	0.77
S	IPI00870234	Gstm6l	Glutathione S-transferase M6-like	Metabolism	Glutathione transferase	0.80
S	IPI00214614	Pabpc3	Poly(A) binding protein, cytoplasmic 3	Metabolism	RNA binding	0.77
S	IPI00231107	Ptms	Parathymosin	Metabolism	DNA replication	0.77
S	IPI00370315	Eif4h	Eukaryotic translation initiation factor 4H	Metabolism	Translation initiation factor	0.82
S	IPI00207665	Ensa	Isoform 1Alpha-endosulfine	Unknown	Receptor binding	0.80
S	IPI00373253	Cadps2	Similar to Ca <sup>2+</sup> -dependent activator for secretion protein 2	Vesicular function	Exocytosis	0.76
S	IPI00563431	G3dsa	Glyceraldehyde 3-phosphate dehydrogenase (Fragment)	Catabolism	Glycolysis	1.20
S	IPI00764535	Arpc2	Actin-related protein 2/3 complex subunit 2	Cytoskeleton	Actin binding	1.19
S	IPI00368301	-	Similar to tubulin, alpha 1	Cytoskeleton	Protein transport	1.68
M	IPI00199771	Slc17a6	Vesicular glutamate transporter 2	Ion transport	Transmitter regulation	1.22
S	IPI00368053	Glod4	Glyoxalase domain-containing protein 4	Metabolism	Mitochondrial enzyme	1.22
S	IPI00365935	Ptges3	Prostaglandin E synthase 3	Metabolism	Fatty acid syntesis	1.45
S	IPI00776830	-	Uncharacterized, HSP90-like/ 47 kDa protein	Metabolism	Protein folding	1.18
S	IPI00204884	-	Uncharacterized, HSP90-like/ 20 kDa protein	Metabolism	Protein folding	1.20
S	IPI00371410	Ubxn1	UBX domain-containing protein 1	Metabolism	Protein binding	1.24
S	IPI00394245	-	Uncharacterized, cyclophilin-like/ 40 kDa protein	Metabolism	Protein folding	1.26
S	IPI00782193	Cltc25	Clathrin heavy chain	Vesicular function	Endocytosis	1.34
S	IPI00387852	Snap91	Synaptosomal-associated protein	Vesicular function	Endocytosis	1.38

TABLE II B

Fraction	IPI number	Abbreviation	Protein description	Function description	Process	R vs A
M	IPI00372040	Arpc4	Actin related protein 2/3 complex, subunit 4	Cytoskeleton	Actin binding	0.78
S	IPI00421723	Tbca	Tubulin-specific chaperone A	Cytoskeleton	Unfolded protein binding	0.81
M	IPI00569279	Hist2h2ab	Histone 2A	Metabolism	Gene regulation	0.60
M	IPI00569391	Tmpo	Thymopoeitin/75 kDa protein	Metabolism	Transcription factor	0.62
M	IPI00395291	Slc1a4	Neutral amino acid transporter ASCT1	Metabolism	Transmembrane transport	0.66
M	IPI00766917	Ptprd	Tyrosine-protein phosphatase delta precursor Rec.-type D	Metabolism	Protein dephosphorylation	0.74
M	IPI00421626	Rps9	Rps9 40S ribosomal protein S9	Metabolism	Peptide synthesis	0.77
M	IPI00209308	Nlgn2	Isoform 1 of Neuroligin-2	Metabolism	Protein binding	0.78
M	IPI00767698	Rab6b	Member RAS oncogene family	Metabolism	Protein binding	0.80
M	IPI00561936	Acly	ATP citrate lyase	Metabolism	Lipid metabolism	0.81
M	IPI00370527	-	Ribosomal_S4/22 kDa protein	Metabolism	Peptide synthesis	0.81
M	IPI00559107	-	Putative uncharacterized protein	Unknown	Unknown	0.69
S	IPI00561103	-	Putative uncharacterized protein	Unknown	Unknown	0.82
M	IPI00188732	Syngn1	Synaptogyrin-1 Isoform CRA_C	Vesicular function	Exocytosis	0.60
M	IPI00205493	Snca	Isoform Syn1 of Alpha-synuclein	Vesicular function	Exocytosis	0.70
S	IPI00362469	Pgls	6-phosphogluconolactonase	Catabolism	Pentose-phosphate shunt	1.27
M	IPI00193233	Cyb5b	Cytochrome b5 type B	Catabolism	Cellular respiration	1.32
S	IPI00211317	Dynll2	Dynein light chain 2, cytoplasmic	Cytoskeleton	Protein transport	1.26

TABLE II B—continued

Fraction	IPI number	Abbreviation	Protein description	Function description	Process	R vs A
M	IPI00476965	Cacna1b	Voltage gated N-type calcium channel Ca(V)2.2	Ion channel	Ion transport	1.24
M	IPI00364599	Cacna1b	Pore-forming calcium channel alpha-1B subunit variant a	Ion channel	Ion transport	1.24
M	IPI00187596	Slc6a1	Sodium- and chloride-dependent GABA transporter 1	Ion transport	Neurotransmitter transport	1.28
M	IPI00829505	Lap3	Isoform 2 of Cytosol aminopeptidase	Metabolism	Protein metabolism	1.22
M	IPI00870183	Cisd1	CDGSH iron sulfur domain-containing protein 1	Metabolism	Cellular respiration	1.22
M	IPI00200552	Rpl26	60S ribosomal protein L26	Metabolism	Peptide synthesis	1.22
S	IPI00362105	Psmc6	Proteasome (prosome, macropain) 26S subunit, ATPase, 6	Metabolism	Nucleotide binding	1.28
M	IPI00205559	Crtac1	Cartilage acidic protein 1	Miscellaneous	Ion binding	1.30
M	IPI00566814	Cd200	OX-2 membrane glycoprotein	Miscellaneous	Protein binding	1.33
M	IPI00476554	Gng2	Guanine nucleotide binding protein gamma 2 (Fragment)	Signal transduction	G-protein signalling	1.27
M	IPI00370116	-	Putative uncharacterized protein	Unknown	Unknown	1.20
M	IPI00212980	-	Isoform Long of Brain protein 44	Unknown	Unknown	1.21
M	IPI00362291	-	Putative uncharacterized protein/16 kDa protein	Unknown	Unknown	1.41
S	IPI00198486	Ap3d1	Adaptor-related protein complex 3, delta 1 subunit	Vesicular function	Protein transport	1.28

TABLE II C

Fraction	IPI number	Abbreviation	Protein description	Function description	Process	C vs R
M	IPI00192246	Cox5a	Cytochrome c oxidase subunit 5A, mitochondrial	Catabolism	Oxidative phosphorylation	0.74
M	IPI00365170	Ndubf7	NADH dehydrogenase (ubiquinone) 1 beta subcomplex, 7	Catabolism	Oxidative phosphorylation	0.77
M	IPI00188330	Ndufs8	NADH dehydrogenase (ubiquinone) Fe-S protein 8	Catabolism	Oxidative phosphorylation	0.78
M	IPI00193918	Cox5b	Cytochrome c oxidase subunit 5B, mitochondrial	Catabolism	Oxidative phosphorylation	0.79
S	IPI00194312	Ola1	Ola1 Obg-like ATPase 1	Catabolism	ATP binding	0.79
M	IPI00201307	Uqcrb	Ubiquinol-cytochrome c reductase binding protein	Catabolism	Oxidative phosphorylation	0.81
S	IPI00362469	Pgls	6-phosphogluconolactonase	Catabolism	Pentose-phosphate shunt	0.81
M	IPI00369419	-	Uncharacterized cofilin-like/19 kDa protein	Cytoskeleton	Actin binding	0.76
M	IPI00364599	Cacna1b	Pore-forming calcium channel alpha-1B subunit variant a	Ion channel	Calcium ion transport	0.74
M	IPI00476965	Cacna1b	Voltage gated N-type calcium channel Ca(V)2.2	Ion channel	Calcium ion transport	0.76
M	IPI00208061	Atp1b3	Sodium/potassium-transporting ATPase subunit beta-3	Ion transport	Sodium/potassium transport	0.81
S	IPI00214614	Pabpc3	Poly(A) binding protein, cytoplasmic 3	Metabolism	RNA binding	0.68
S	IPI00189074	Pabpc1	Polyadenylate-binding protein 1	Metabolism	RNA binding	0.76
M	IPI00231771	S100b	S100 calcium binding protein B	Miscellaneous	Protein binding	0.71
M	IPI00476554	Gng2	Guanine nucleotide binding protein gamma 2 (Fragment)	Signal transduction	G-protein signalling	0.82
M	IPI00362291	-	Putative uncharacterized protein/16 kDa protein	Unknown	Unknown	0.69
M	IPI00566858	-	Putative uncharacterized protein/37 kDa protein	Catabolism	Glycolysis	1.22
M	IPI00569391	Tmpo	Thymopoetin/75 kDa protein	Metabolism	Transcription factor	1.33
S	IPI00373214	Kpna4	Karyopherin alpha 4	Miscellaneous	Protein transport	1.21

ceptible and stress-resilient phenotypes in rats. The CA region was chosen because of its association to cognitive function (35–37) and the profound effects seen in this region in

response to stress (38). The macro-dissection method used was designed to obtain the CA-regions (21) and no further distinction of the CA region into CA1 and CA3 was applied.

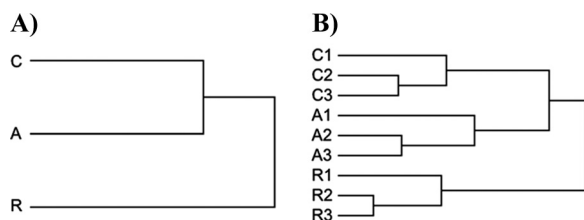


FIG. 4. Hierarchical cluster analysis performed on data from all 2011 proteins (A) and on the 75 proteins that passed selection criteria (B). According to both cluster profiles the resilient (R) group diverged from the anhedonic (A) and the control (C) group demonstrating that the CMS-resilient protein expression profile differed from the other two groups investigated.

Cluster analysis on all proteins indicated that, in terms of protein expression levels in the CA-region, resilient rats had a distinct proteome profile (Fig. 4). These findings agree with a microarray study on the nucleus accumbens and the ventral tegmental area in socially-defeated mice (39). Previously, we found by hierarchical clustering analysis that the anhedonic group co-segregates with unchallenged controls in a subcluster diverging from a subcluster including resilient rats and escitalopram-responder rats (20). It seems that the coping mechanisms associated to the resilience phenotype implies a high degree of molecular adaptations across several brain regions.

A range of both preclinical and clinical studies has shown the hippocampal region to be affected in depressed subjects, without showing direct causal linkage (40, 41). These studies have given rise to investigations on potential molecular pathways and targets that could explain these effects, pointing to neurotrophines such as BDNF and VEGF (42, 43), or proteins involved in the cyclic-AMP pathway (44). However, as with the anatomical effects, no direct causal relation has been established between a given protein, or molecular pathway, and depressive behavior. Given this lack of knowledge on specific proteins and pathways associated to depression, we used a general, hypothesis-generating bioinformatic approach to search for novel molecular targets potentially involved in the pathology of depression. Based on Panther (45), Ingenuity, and Pubmed searches, some of these proteins were selected for more detailed description with respect to function and possible relation to depression.

To validate the group protein regulation patterns a validation study was conducted, using material from new rat specimens (nine rats from each treatment group) prepared with the same procedures as in the main large scale proteomics study. In general there was a good correlation between the iTRAQ data and SRM data, but three proteins did not show comparable group regulation patterns. This could be because of false positives, or a potential regulation could be masked by biological variation. Consequently conclusions based on these proteins should be taken with caution.

Comparing the control and anhedonic rats, 22 proteins passed significance criteria. Ingenuity pathway analysis re-

vealed a number of proteins of potential interest to psychiatric disorders in general, but also specifically with respect to depressive disorder.

The sodium-channel protein SCN9A (also referred to as Nav1.7) was significantly up-regulated (23%) in the anhedonic group compared with controls. Concurrently the SCN9A-expression level was 21% higher in the anhedonic group compared with resilient, but this difference was only borderline significant ( $p = 0.07$ ). SCN9A is a voltage-gated sodium channel, important for the generation and conductance of action potentials and studies have shown that SCN9A plays a central role in pain sensing (46, 47). Moreover, riluzole, a drug blocking tetrodotoxin-sensitive sodium channels including SCN9A, was found to have to have antidepressant action (48). Hippocampal SCN9A expression was confirmed by immunohistochemical staining. Mainly in the CA1 region the immunoreactivity was observed to be higher in anhedonic rats compared with controls (Fig. 6). This observation confirmed the results from the proteomics data and points to a region-specific up-regulation of this protein. We speculate that up-regulation of SCN9A may contribute to a stress-susceptible phenotype.

The calcium-dependent activator for secretion protein 2 (CADPS2) was significantly up-regulated (24%) in the anhedonic group compared with controls. CADPS is involved in regulating exocytosis at dense core vesicles (49). Moreover, CADPS2 plays a role in sleeping patterns and is a critical protein in the differentiation of hippocampal neurons (50). Although the literature does not provide direct linkage between CADPS2 and depression, a disrupted sleeping pattern is a common symptom of depression (51). Moreover, hippocampal neurogenesis and differentiation may be linked with depression (43), suggesting that stress-induced perturbed CADPS2 levels may occur in depressive disorder. Interestingly, the *Cadps2* gene has also been associated with bipolar disorder (52).

The alpha-endosulfine (ENSA) protein was significantly up-regulated (20%) in the anhedonic group compared with controls. The role of ENSA in brain function is not well-established, but a stress-induced up-regulation of ENSA has previously been reported in rats following swim-stress (53). In addition, Dou and colleagues report a neurotoxicity-induced up-regulation of ENSA following streptozocin injection. Based on these findings, one could speculate that ENSA plays a role in stress-induced neuronal atrophy.

Clathrin coat assembly protein (SNAP91 or AP180) was significantly down-regulated (38%) in the anhedonic group compared with control. SNAP91 has been shown to be important for synaptic vesicle recycling (54, 55) and may be implicated in psychiatric disorders such as schizophrenia and bipolar disorder by imposing a deficit in vesicular turnover (56, 57).

Comparing resilient and anhedonic rats, 32 proteins passed significance criteria. Among these proteins, several are in-



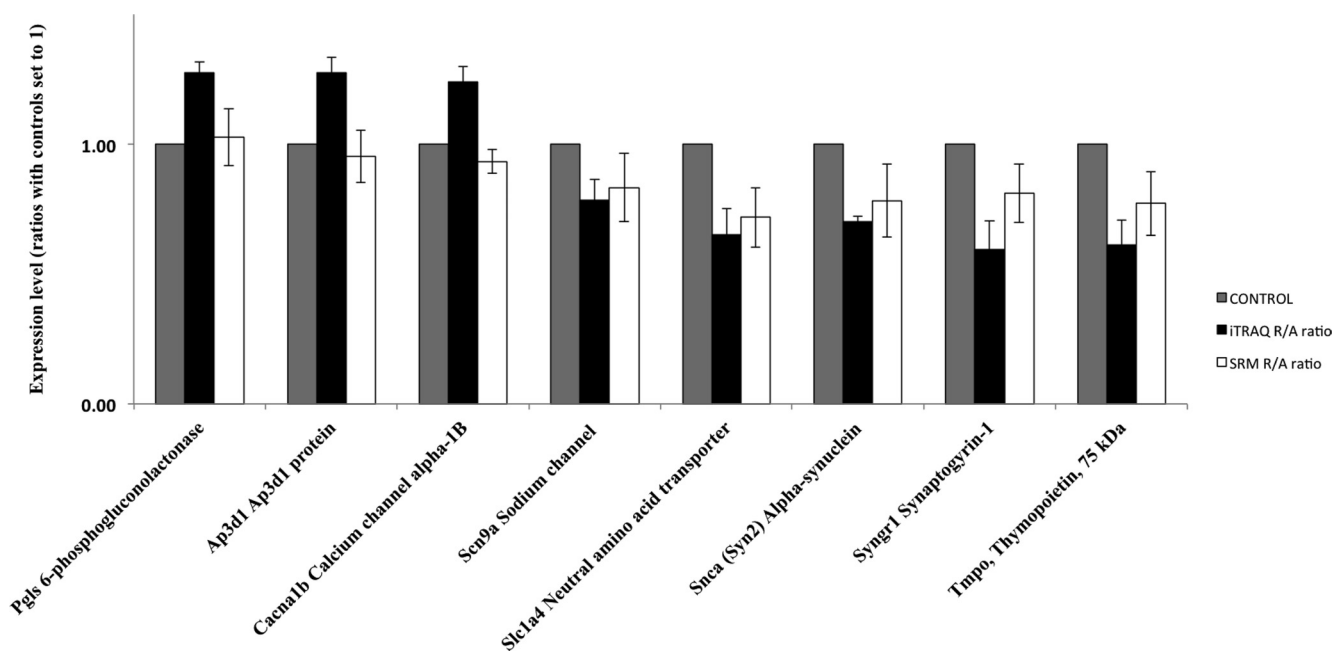


FIG. 5. Expression level comparison between data obtained in original experiment using iTRAQ labeling and validation study using the SRM method.

involved in vesicular function thus indicating that alterations in neurotransmission might underlie resiliency. For example, alpha-synuclein (SNCA) was significantly down-regulated (30%) in the resilient group as compared with the anhedonic group. SNCA is expressed throughout the brain, but has been shown to be enriched in presynaptic terminals (58). Moreover, SNCA is involved in synaptic plasticity and neurotransmission, potentially through regulating vesicle density by inhibiting exocytosis (59, 60). In addition, SNCA is involved in Parkinson disease as a major constituent in the development of Lewy bodies (61). Its relation to depression is not well-established, but the comorbidity of Parkinson disease and depression is high (62). Further, a recent study found SNCA mRNA was correlated to scores obtained on the Beck depression inventory (63).

Synaptogyrin 1 (SYN-1) is another protein involved in vesicular function and, like SNCA, SYN-1 regulates vesicle density by inhibiting exocytosis (64). The expression level of SYN-1 was also decreased (40%) in resilient rats compared with anhedonic rats. In line with the results regarding SNCA and SYN-1 levels and their potential regulation of exocytosis, a recent study on zinc-deficient mice showed that susceptibility to stress associates with a decrease in exocytosis (65). In addition to SNCA and SYN-1, the adaptor-related protein complex 3 (AP-3) plays a potential role in vesicular function; mice lacking the AP-3 protein have decreased density of synaptic vesicles at inhibitory terminals in the CA1 region (66). The AP-3 protein was significantly up-regulated (28%) in the resilient group compared with the anhedonic group ( $p = 0.04$ ). It has to be noted that the group expression pattern of AP-3 was not confirmed in the validation study. In addition to the above-mentioned proteins several pro-

teins involved in vesicular functions are differentially expressed between the three groups further emphasizing that this biological function is affected by stress.

In support of a theory on CMS-induced alterations of vesicular-related proteins, a recent study on punches of dentate gyrus tissue from CMS-exposed rats also showed alterations in vesicular-related proteins (67). Moreover, an earlier study at our facility likewise identified differentially expressed vesicular-related proteins in rat hippocampus following stress exposure (20).

We speculate that a general hippocampal deficit in vesicular function in anhedonic rats has implications that might explain previously reported results on anhedonic rats, showing a significantly decreased number of miniature inhibitory postsynaptic potentials and a reduced GABA release probability (11). In support of this theory, a study on the role of SNCA showed a significant decrease in the frequency of miniature excitatory postsynaptic potentials in mice overexpressing human SNCA (68). Furthermore, the decrease in hippocampal GABA levels seen in studies on mice exposed to CMS could also be explained by a deficit in vesicular function (69, 70).

In future studies it will be interesting to elucidate whether stress-tolerance-specific alterations of SNCA and other vesicular-related proteins is a general neuromolecular mechanism, or whether this regulation is restricted to the hippocampus.

Comparing resilient and control rats, 19 proteins passed significance criteria. Most cell energy is obtained through oxidative phosphorylation and it is well known that brain tissue has a high energy demand. Studies have shown that chronic stress affects the mitochondrial respiratory chain and several studies have proposed mitochondrial dysfunction as a potential mechanism

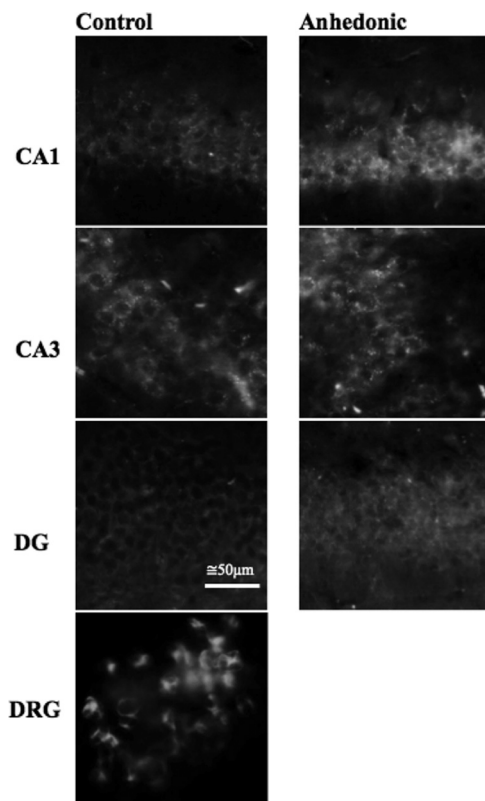


**FIG. 6. Sagittal SCN9A-stained brain slices of the hippocampus showed increased immunoreactivity in anhedonic rats compared with controls, especially pronounced in the CA1 region.** Immunoreactivity was lowest in the dentate gyrus (DG). Immunoreactivity was confirmed in sections of dorsal root ganglion (DRG), known to have a large density of sodium channels.

underlying the pathophysiology of psychiatric disorders (71, 72). Five proteins involved in oxidative phosphorylation were significantly up-regulated in the resilient group compared with controls, namely COX5A, NDUFB7, NDUFS8, COX5B, and UQCRCB. For all five proteins the expression in stress-susceptible rats was intermediate between control and resilient, thus it could be speculated that the regulation of these proteins provides protection against stress, but in the stress-susceptible rats the level of regulation is insufficient. We speculate that increased oxidative phosphorylation is an adaptive and protective mechanism underlying a stress-resilient phenotype. It could be argued that increased oxidative phosphorylation is caused by increased physical activity, however this is not supported by our study showing that increased locomotion is not specifically associated to the resilient group rather it associates to stress exposure in general which we also have observed in previous studies (17). We have seen the same association between stress exposure and locomotor activity when working with open field tests (unpublished).

Four proteins are coregulated in the R versus A and R versus C comparisons, namely TMPO, PGLS, CACNA1b (two isoforms), and GNG2. These proteins comply with a model of the resilient group as having a specific phenotypic response to

stress, segregating away from the control and the anhedonic group. TMPO (thymopoietin) has been proposed to be involved in stress responses associated with depression and has been shown to be up-regulated in blood plasma of depressed patients, specifically patients unresponsive to antidepressant treatment (73). Interestingly, the resilient group showed a (38%) down-regulation of TMPO compared with the anhedonic group and a (33%) down-regulation compared with controls, in support of a potential role of TMPO in stress-induced depression. PGLS (6-phosphogluconolactonase) is a protein involved in the pentose phosphate shunt. PGLS was (27%) up-regulated in the resilient group compared with the anhedonic group and (19%) up-regulated compared with controls. Because an increased pentose phosphate shunt could prevent oxidative stress, it could be speculated that the increased expression levels of PGLS in the resilient group is a stress protective mechanism. CACNA1b is a voltage dependent calcium channel involved in neurotransmitter release. CACNA1b was (23%) and (24%) up-regulated in the resilient group compared with the anhedonic and control group respectively. Increased levels of CACNA1b could serve to increase hippocampal neurotransmission in the resilient group, as a way to compensate for the decrease in neurotransmission shown following exposure to chronic stress (74). It has to be noted that the group expression pattern of CACNA1b was not confirmed in the validation study. GNG2 does, to our knowledge, not have any previously known association to chronic stress or depression.

In summary, our unbiased proteome-wide approach identified several candidate proteins that may be related to stress-susceptibility and stress-resilience. Regarding stress-susceptibility, we found the sodium channel SCN9A to be up-regulated in stress-susceptible rats. Based on previous studies, we propose that SCN9A may be a potential novel biomarker of depression. Based on the results in the stress-resilient rats, we propose that the conservation of vesicular functioning is central in stress coping strategies. Finally, our results indicate that increased oxidative phosphorylation within the hippocampal CA regions may be important in resistance to stress.

*Acknowledgments*—We thank Stine Dhiin Heide for her skilled animal handling and care, and Dr Donald Smith for valuable text editing.

\* This work was supported by the Lundbeck Foundation, the Augustinus Foundation, and the John and Birthe Meyer Foundation.

§ This article contains [supplemental material](#).

|| To whom correspondence should be addressed: Centre for Psychiatric Research, Brendstrupgaardsvej 102, 8200 Aarhus N, Denmark, Tel +45 86 20 52 47 Fax +45 86 20 12 28; kimhenni@rm.dk.

\*\* Contributed equally to this work.

Kim Henningsen, kimhenni@rm.dk; Johan Palmfeldt, johan.palmfeldt@ki.au.dk; Sofie Christiansen, sofie.christiansen@gmail.com; Steffen Bak, stbak@health.sdu.dk; Isabel Baiges, isabel.baiges@urv.cat; Niels Gregersen, nig@ki.au.dk; Ove Wiborg, owiborg@post.tele.dk.

## REFERENCES

- Kessler, R. C. (1997) The effects of stressful life events on depression. *Annu. Rev. Psychol.* **48**, 191–214
- Green, K. T., Calhoun, P. S., Dennis, M. F., and Beckham, J. C. (2010) Exploration of the resilience construct in posttraumatic stress disorder severity and functional correlates in military combat veterans who have served since September 11, 2001. *J. Clin. Psychiatry* **71**, 823–830
- Kendler, K. S., Karkowski, L. M. and Prescott, C. A. (1999) Causal relationship between stressful life events and the onset of major depression. *Am. J. Psychiatry* **156**, 837–841
- Hjemdal, O., Vogel, P. A., Solem, S., Hagen, K., and Stiles, T. C. (2010) The relationship between resilience and levels of anxiety, depression, and obsessive-compulsive symptoms in adolescents. *Clin. Psychol. Psychother.* **18**, 314–321
- Haefel, G. J., and Vargas, I. (2011) Resilience to depressive symptoms: The buffering effects of enhancing cognitive style and positive life events. *J. Behav. Ther. Exp. Psychiatry* **42**, 13–18
- McEwen, B. S. (2000) The neurobiology of stress: from serendipity to clinical relevance. *Brain Res.* **886**, 172–189
- Sapolsky, R. M. (2000) Glucocorticoids and hippocampal atrophy in neuropsychiatric disorders. *Arch. Gen. Psychiatry* **57**, 925–935
- McIntyre, C. K., Power, A. E., Roozendaal, B., and McGaugh, J. L. (2003) Role of the basolateral amygdala in memory consolidation. *Ann. N.Y. Acad. Sci.* **985**, 273–293
- Roozendaal, B., Hahn, E. L., Nathan, S. V., de Quervain, D. J., and McGaugh, J. L. (2004) Glucocorticoid effects on memory retrieval require concurrent noradrenergic activity in the hippocampus and basolateral amygdala. *J. Neurosci.* **24**, 8161–8169
- Sheline, Y. I., (2000) 3D MRI studies of neuroanatomic changes in unipolar major depression: the role of stress and medical comorbidity. *Biol. Psychiatry* **48**, 791–800
- Holm, M. M., Nieto-Gonzalez, J. L., Vardya, I., Henningsen, K., Jayatissa, M. N., Wiborg, O., and Jensen, K. (2010) Hippocampal GABAergic dysfunction in a rat chronic mild stress model of depression. *Hippocampus* **21**, 422–433
- Nestler, E. J., Barrot, M., DiLeone, R. J., Eisch, A. J., Gold, S. J., and Monteggia, L. M. (2002) Neurobiology of depression. *Neuron*, **34**, 13–25
- Katz, R. J., and Baldrighi, G. (1982) A further parametric study of imipramine in an animal model of depression. *Pharmacol. Biochem. Behav.* **16**, 969–972
- Willner, P., Towell, A., Sampson, D., Sophokleous, S., and Muscat, R. (1987) Reduction of sucrose preference by chronic unpredictable mild stress, and its restoration by a tricyclic antidepressant. *Psychopharmacology (Berl)* **93**, 358–364
- Willner, P. (1997) Validity, reliability and utility of the chronic mild stress model of depression: a 10-year review and evaluation. *Psychopharmacology* **134**, 319–329
- Banasr, M., Chowdhury, G. M., Terwilliger, R., Newton, S. S., Duman, R. S., Behar, K. L., and Sanacora, G. (2010) Glial pathology in an animal model of depression: reversal of stress-induced cellular, metabolic and behavioral deficits by the glutamate-modulating drug riluzole. *Mol. Psychiatry* **15**, 501–511
- Henningsen, K., Andreassen, J. T., Bouzinova, E. V., Jayatissa, M. N., Jensen, M. S., Redrobe, J. P., and Wiborg, O. (2009) Cognitive deficits in the rat chronic mild stress model for depression: relation to anhedonic-like responses. *Behav. Brain Res.* **198**, 136–141
- Moreau, J. L., Scherschlicht, R., Jenck, F., and Martin, J. R. (1995) Chronic mild stress-induced anhedonia model of depression; sleep abnormalities and curative effects of electroshock treatment. *Behav. Pharmacol.* **6**, 682–687
- Bergström, A., Jayatissa, M. N., Mork, A., and Wiborg, O. (2008) Stress sensitivity and resilience in the chronic mild stress rat model of depression; an in situ hybridization study. *Brain Res.* **1196**, 41–52
- Bisgaard, C. F., Jayatissa, M. N., Enghild, J. J., Sánchez, C., Artemychn, R., and Wiborg, O. (2007) Proteomic investigation of the ventral rat hippocampus links DRP-2 to escitalopram treatment resistance and SNAP to stress resilience in the chronic mild stress model of depression. *J. Mol. Neurosci.* **32**, 132–144
- Lein, E. S., Zhao, X., and Gage, F. H. (2004) Defining a molecular atlas of the hippocampus using DNA microarrays and high-throughput in situ hybridization. *J. Neurosci.* **24**, 3879–3889
- Fujiki, Y., Hubbard, A. L., Fowler, S., and Lazarow, P. B. (1982) Isolation of intracellular membranes by means of sodium carbonate treatment: application to endoplasmic reticulum. *J. Cell Biol.* **93**, 97–102
- Bordier, C. (1981) Phase separation of integral membrane proteins in Triton X-114 solution. *J. Biol. Chem.* **256**, 1604–1607
- Moebius, J., Zahedi, R. P., Lewandrowski, U., Berger, C., Walter, U., and Sickmann, A. (2005) The human platelet membrane proteome reveals several new potential membrane proteins. *Mol. Cell. Proteomics* **4**, 1754–1761
- Baiges, I., Palmfeldt, J., Bladé, C., Gregersen, N., and Arola, L. (2010) Lipogenesis is decreased by grape seed proanthocyanidins according to liver proteomics of rats fed a high fat diet. *Mol. Cell. Proteomics* **9**, 1499–1513
- Vizcaino, J. A., Côté, R., Reisinger, F., Barsnes, H., Foster, J. M., Rameseder, J., Hermjakob, H., and Martens, L. (2010) The Proteomics Identifications database: 2010 update. *Nucleic Acids Res.* **38**, D736–742
- Benjamini, Y., Drai, D., Elmer, G., Kafkafi, N., and Golani, I. (2001) Controlling the false discovery rate in behavior genetics research. *Behav. Brain Res.* **125**, 279–284
- Carvalho, P. C., Fischer, J. S., Chen, E. I., Yates, J. R., 3rd, and Barbosa, V. C. (2008) PatternLab for proteomics: a tool for differential shotgun proteomics. *BMC Bioinformatics* **9**, 316
- Eisen, M. B., Spellman, P. T., Brown, P. O., and Botstein, D. (1998) Cluster analysis and display of genome-wide expression patterns. *Proc. Natl. Acad. Sci. U.S.A.* **95**, 14863–14868
- Bergström, A., Jayatissa, M. N., Thykjaer, T., and Wiborg, O. (2007) Molecular pathways associated with stress resilience and drug resistance in the chronic mild stress rat model of depression: a gene expression study. *J. Mol. Neurosci.* **33**, 201–215
- Southwick, S. M., Vythilingam, M., and Charney, D. S. (2005) The psychobiology of depression and resilience to stress: implications for prevention and treatment. *Annu. Rev. Clin. Psychol.* **1**, 255–291
- Feder, A., Nestler, E. J., and Charney, D. S. (2009) Psychobiology and molecular genetics of resilience. *Nat. Rev. Neurosci.* **10**, 446–457
- Vialou, V., Robison, A. J., Laplant, Q. C., Covington, H. E., 3rd, Dietz, D. M., Ohnishi, Y. N., Mouzon, E., Rush, A. J., 3rd, Watts, E. L., Wallace, D. L., Iniguez, S. D., Ohnishi, Y. H., Steiner, M. A., Warren, B. L., Krishnan, V., Bolanos, C. A., Neve, R. L., Ghose, S., Berton, O., Tamminga, C. A., and Nestler, E. J. (2010) DeltaFosB in brain reward circuits mediates resilience to stress and antidepressant responses. *Nat. Neurosci.* **13**, 745–752
- Drugan, R. C., Christianson, J. P., Stine, W. W., and Soucy, D. P. (2009) Swim stress-induced ultrasonic vocalizations forecast resilience in rats. *Behav. Brain Res.* **202**, 142–145
- Wagatsuma, H., and Yamaguchi, Y. (2007) Neural dynamics of the cognitive map in the hippocampus. *Cogn. Neurodyn.* **1**, 119–141
- Gold, A. E., and Kesner, R. P. (2005) The role of the CA3 subregion of the dorsal hippocampus in spatial pattern completion in the rat. *Hippocampus* **15**, 808–814
- Hunsaker, M. R., Thorup, J. A., Welch, T., and Kesner, R. P. (2006) The role of CA3 and CA1 in the acquisition of an object-trace-place paired-associate task. *Behav. Neurosci.* **120**, 1252–1256
- McEwen, B. S., and Sapolsky, R. M. (1995) Stress and cognitive function. *Curr. Opin. Neurobiol.* **5**, 205–216
- Krishnan, V., Han, M. H., Graham, D. L., Berton, O., Renthall, W., Russo, S. J., Laplant, Q., Graham, A., Lutter, M., Lagace, D. C., Ghose, S., Reister, R., Tannous, P., Green, T. A., Neve, R. L., Chakravarty, S., Kumar, A., Eisch, A. J., Self, D. W., Lee, F. S., Tamminga, C. A., Cooper, D. C., Gershenfeld, H. K., and Nestler, E. J. (2007) Molecular adaptations underlying susceptibility and resistance to social defeat in brain reward regions. *Cell* **131**, 391–404
- Sheline, Y. I. (2003) Neuroimaging studies of mood disorder effects on the brain. *Biol. Psychiatry* **54**, 338–352
- Harrison, P. J. (2002) The neuropathology of primary mood disorder. *Brain* **125**, 1428–1449
- Monteggia, L. M., Barrot, M., Powell, C. M., Berton, O., Galanis, V., Gemelli, T., Meuth, S., Nagy, A., Greene, R. W., and Nestler, E. J. (2004) Essential role of brain-derived neurotrophic factor in adult hippocampal function. *Proc. Natl. Acad. Sci. U.S.A.* **101**, 10827–10832
- Duman, R. S., and Monteggia, L. M. (2006) A neurotrophic model for stress-related mood disorders. *Biol Psychiatry* **59**, 1116–1127
- Pittenger, C., and Duman, R. S. (2008) Stress, depression, and neuroplas-

- ticity: a convergence of mechanisms. *Neuropsychopharmacology* **33**, 88–109
45. Thomas, P. D., Campbell, M. J., Kejarawal, A., Mi, H., Karlak, B., Daverman, R., Diemer, K., Muruganujan, A., and Narechania, A. (2003) PANTHER: a library of protein families and subfamilies indexed by function. *Genome Res.* **13**, 2129–2141
  46. Goldberg, Y. P., MacFarlane, J., MacDonald, M. L., Thompson, J., Dube, M. P., Mattice, M., Fraser, R., Young, C., Hossain, S., Pape, T., Payne, B., Radomski, C., Donaldson, G., Ives, E., Cox, J., Youngusband, H. B., Green, R., Duff, A., Boltshauser, E., Grinspan, G. A., Dimon, J. H., Sibley, B. G., Andria, G., Toscano, E., Kerdraon, J., Bowsher, D., Pimstone, S. N., Samuels, M. E., Sherrington, R., and Hayden, M. R. (2007) Loss-of-function mutations in the Nav1.7 gene underlie congenital indifference to pain in multiple human populations. *Clin. Genet.* **71**, 311–319
  47. Nassar, M. A., Stirling, L. C., Forlani, G., Baker, M. D., Matthews, E. A., Dickenson, A. H., and Wood, J. N. (2004) Nociceptor-specific gene deletion reveals a major role for Nav1.7 (PN1) in acute and inflammatory pain. *Proc. Natl. Acad. Sci. U.S.A.* **101**, 12706–12711
  48. Zarate, C. A., Jr., Payne, J. L., Quiroz, J., Sporn, J., Denicoff, K. K., Luckenbaugh, D., Charney, D. S., and Manji, H. K. (2004) An open-label trial of riluzole in patients with treatment-resistant major depression. *Am. J. Psychiatry* **161**, 171–174
  49. Grishanin, R. N., Kowalchuk, J. A., Klenchin, V. A., Ann, K., Earles, C. A., Chapman, E. R., Gerona, R. R., and Martin, T. F. (2004) CAPS acts at a prefusion step in dense-core vesicle exocytosis as a PIP2 binding protein. *Neuron* **43**, 551–562
  50. Sadakata, T., Washida, M., Iwayama, Y., Shoji, S., Sato, Y., Ohkura, T., Katoh-Semba, R., Nakajima, M., Sekine, Y., Tanaka, M., Nakamura, K., Iwata, Y., Tsuchiya, K. J., Mori, N., Detera-Wadleigh, S. D., Ichikawa, H., Itohara, S., Yoshikawa, T., and Furuichi, T. (2007) Autistic-like phenotypes in Cadps2-knockout mice and aberrant CADPS2 splicing in autistic patients. *J. Clin. Invest.* **117**, 931–943
  51. Hasler, G., Drevets, W. C., Manji, H. K., and Charney, D. S. (2004) Discovering endophenotypes for major depression. *Neuropsychopharmacology* **29**, 1765–1781
  52. Palo, O. M., Soronen, P., Silander, K., Varilo, T., Tuononen, K., Kieseppe, T., Partonen, T., Lonnqvist, J., Paunio, T., and Peltonen, L. (2010) Identification of susceptibility loci at 7q31 and 9p13 for bipolar disorder in an isolated population. *Am. J. Med. Genet. B* **153**, 723–735
  53. Dou, J., Cui, C., Dufour, F., Alkon, D. L., and Zhao, W. Q. (2003) Gene expression of alpha-endosulfine in the rat brain: correlative changes with aging, learning and stress. *J. Neurochem.* **87**, 1086–1100
  54. Morgan, J. R., Zhao, X., Womack, M., Prasad, K., Augustine, G. J., and Lafer, E. M. (1999) A role for the clathrin assembly domain of AP180 in synaptic vesicle endocytosis. *J. Neurosci.* **19**, 10201–10212
  55. Granseth, B., Odermatt, B., Royle, S. J., and Lagnado, L. (2006) Clathrin-mediated endocytosis is the dominant mechanism of vesicle retrieval at hippocampal synapses. *Neuron* **51**, 773–786
  56. Chan, M. K., Tsang, T. M., Harris, L. W., Guest, P. C., Holmes, E., and Bahn, S. (2010) Evidence for disease and antipsychotic medication effects in post-mortem brain from schizophrenia patients. *Mol. Psychiatry* **16**, 1189–1202
  57. Hennah, W., and Porteous, D. (2009) The DISC1 pathway modulates expression of neurodevelopmental, synaptogenic and sensory perception genes. *PLoS One* **4**, e4906
  58. Goedert, M., (2001) Alpha-synuclein and neurodegenerative diseases. *Nat. Rev. Neurosci.* **2**, 492–501
  59. Nemani, V. M., Lu, W., Berge, V., Nakamura, K., Onoa, B., Lee, M. K., Chaudhry, F. A., Nicoll, R. A., and Edwards, R. H. (2010) Increased expression of alpha-synuclein reduces neurotransmitter release by inhibiting synaptic vesicle recluster after endocytosis. *Neuron*, **65**, 66–79
  60. Di Rosa, G., Puzzo, D., Sant'Angelo, A., Trinchese, F., and Arancio, O. (2003) Alpha-synuclein: between synaptic function and dysfunction. *Histol. Histopathol.* **18**, 1257–1266
  61. Spillantini, M. G., Schmidt, M. L., Lee, V. M., Trojanowski, J. Q., Jakes, R., and Goedert, M. (1997) Alpha-synuclein in Lewy bodies. *Nature* **388**, 839–840
  62. Frisina, P. G., Haroutunian, V., and Libow, L.S. (2009) The neuropathological basis for depression in Parkinson's disease. *Parkinsonism Related Disorders* **15**, 144–148
  63. Frieling, H., Gozner, A., Römer, K. D., Wilhelm, J., Hillemacher, T., Kornhuber, J., de Zwaan, M., Jacoby, G. E., and Bleich, S. (2008) Alpha-synuclein mRNA levels correspond to beck depression inventory scores in females with eating disorders. *Neuropsychobiology* **58**, 48–52
  64. Sugita, S., Janz, R., and Südhof, T. C. (1999) Synaptogyrins regulate Ca2+-dependent exocytosis in PC12 cells. *J. Biol. Chem.* **274**, 18893–18901
  65. Watanabe, M., Tamano, H., Kikuchi, T., and Takeda, A. (2010) Susceptibility to stress in young rats after 2-week zinc deprivation. *Neurochem. Int.* **56**, 410–416
  66. Nakatsu, F., Okada, M., Mori, F., Kumazawa, N., Iwasa, H., Zhu, G., Kasagi, Y., Kamiya, H., Harada, A., Nishimura, K., Takeuchi, A., Miyazaki, T., Watanabe, M., Yuasa, S., Manabe, T., Wakabayashi, K., Kaneko, S., Saito, T., and Ohno, H. (2004) Defective function of GABA-containing synaptic vesicles in mice lacking the AP-3B clathrin adaptor. *J. Cell Biol.* **167**, 293–302
  67. Kedracka-Krok, S., Fic, E., Jankowska, U., Jaciuk, M., Gruca, P., Papp, M., Kusmider, M., Solich, J., Debski, J., Dadlez, M., and Dziedzicka-Wasylewska, M. (2010) Effect of chronic mild stress and imipramine on the proteome of the rat dentate gyrus. *J. Neurochem.* **113**, 848–859
  68. Scott, D. A., Tabarean, I., Tang, Y., Cartier, A., Masliah, E., and Roy, S. (2010) A pathologic cascade leading to synaptic dysfunction in alpha-synuclein-induced neurodegeneration. *J. Neurosci.* **30**, 8083–8095
  69. Garcia-Garcia, A. L., Elizalde, N., Matrov, D., Harro, J., Wojcik, S. M., Venzala, E., Ramirez, M. J., Del Rio, J., and Tordera, R. M. (2009) Increased vulnerability to depressive-like behavior of mice with decreased expression of VGLUT1. *Biol. Psychiatry* **66**, 275–282
  70. Elizalde, N., Garcia-Garcia, A. L., Totterdell, S., Gendive, N., Venzala, E., Ramirez, M. J., Del Rio, J., and Tordera, R. M. (2010) Sustained stress-induced changes in mice as a model for chronic depression. *Psychopharmacology* **210**, 393–406
  71. Rezin, G. T., Amboni, G., Zugno, A. I., Quevedo, J., and Streck, E. L. (2009) Mitochondrial dysfunction and psychiatric disorders. *Neurochem. Res.* **34**, 1021–1029
  72. Gardner, A., Johansson, A., Wibom, R., Nennesmo, I., von Döbeln, U., Hagenfeldt, L., and Hällström, T. (2003) Alterations of mitochondrial function and correlations with personality traits in selected major depressive disorder patients. *J. Affect. Disord.* **76**, 55–68
  73. Goldstein, G., Fava, M., Culler, M., Fisher, A., Rickels, K., Lydiard, R. B., and Rosenbaum, J. (2000) Elevated plasma thymopoietin associated with therapeutic nonresponsiveness in major depression. *Biol. Psychiatry* **48**, 65–69
  74. Alfarez, D. N., Joëls, M., and Krugers, H. J. (2003) Chronic unpredictable stress impairs long-term potentiation in rat hippocampal CA1 area and dentate gyrus in vitro. *Eur. J. Neurosci.* **17**, 1928–1934